

Research and Application of Parallel Mismatch Detection and Reconfiguration Method for Photovoltaic (PV) Arrays

Shuai Sun, Ping Yun, Xuebing Chen, Peng Chen
Sungrow Power Supply Co., LTD. Hefei 230088, China

Abstract: To solve the problem of generation loss caused by photovoltaic (PV) array parallel mismatch, this paper proposes a reconstruction method using short-time I - V curve scan detection and based on the root mean square of the difference of V_{mp} (maximum power point voltage). First, the short-time I - V curve scan is applied to obtain the V_{mp} distribution characteristics of each PV array, and then the optimal reconstruction results are output using the root mean square of the V_{mp} difference between each PV array. Subsequently, the basic principles of the above methods are introduced, and a PV power station test platform with a capacity of 125KW is built. The test results on the platform show that the proposed methods can significantly reduce the power loss caused by mismatch, which validates the effectiveness of the methods described in this paper.

Keywords: PV Display; Parallel Mismatch; IV Scan; Root Mean Square of Difference; Power Loss

Introduction

Most photovoltaic (PV) power stations are in good condition at the initial stage of operation, but with the increase of operating years, PV modules often suffer from aging, dusty, cracked, potential-induced degradation (PID) effect, shadow shielding and inconsistent open circuit voltage. All of the above will lead to the parallel mismatch (all the mismatches described later in this paper are parallel mismatches between PV arrays) of PV arrays (composed of multiple PV modules in series), thus causing the loss of PV power generation^[1-3]. Therefore, solving the mismatch problem is the key to improve the power generation of PV power plants. At present, the commonly used detection method is dispersion rate analysis, which can evaluate the current consistency of PV array^[4-5], but fails to explain the problem from the perspective of internal mechanism. In practice, the two PV arrays interact with each other, and it is easy to cause misjudgment through dispersion rate analysis, especially after reconstruction, which is very easy to further deepen the mismatch. Thus, based on the mechanism of parallel mismatch, this paper proposes a method of parallel mismatch detection and reconstruction for PV arrays. This method does not need to add any hardware equipment, and is only realized by the software algorithm of the internal controller of the inverter, with high accuracy.

1. Mechanism analysis of PV array parallel mismatch

1.1 Equivalent model for photovoltaic cells

The equivalent circuit model of photovoltaic cells can be described by single- and double-diode models^[6], but the model does not consider the influence of parasitic parameters, so a series resistor R_s with a shunt resistor R_{sh} and a parallel diode I_d are added to the equivalent model circuit in this paper. The corresponding I - V curve equation is expressed as equation (1). This equivalent circuit model can be used not only for PV modules including multiple batteries, but also for PV arrays including multiple PV modules^[7].

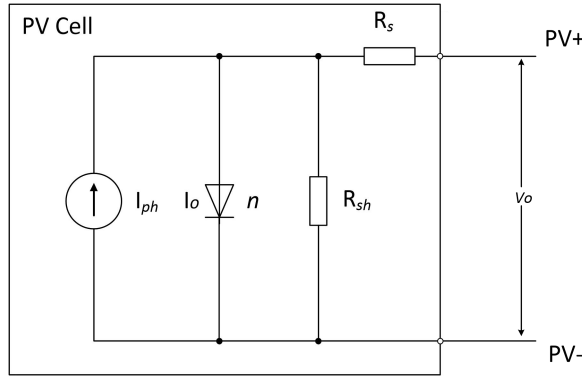


Figure 1. Equivalent model of the photovoltaic cell

$$I = I_{ph} - I_o \left[\exp \left(\frac{V + IR_s}{nV_{th}} \right) - 1 \right] - \frac{V + IR_s}{R_{sh}} \quad (1)$$

In the above equation n is the diode ideal factor and $V_{th} = kT/q$ is the thermoelectric force, where k is the Boltzmann constant and T is the absolute temperature.

1.2 Mechanism analysis of PV array parallel mismatch

The mismatch loss of PV arrays actually includes the series mismatch loss of PV components in the array and the parallel mismatch loss between PV arrays. This paper mainly analyzes the parallel mismatch and its loss.

Firstly, the parallel connection of two PV modules is taken as the analysis object, and the mismatch mechanism is analyzed. In a parallel circuit, the voltage V_i of each PV module is equal to the voltage V after parallel connection, so the power equation of each PV module can be expressed by the voltage^[8]:

$$P_i = -\frac{V^2}{R_{si}} + \frac{n_i V V_{th}}{R_{si}} \left[-W(X_i) + \frac{R_{shi}(R_{si}I_{phi} + R_{si}I_{oi} + V)}{n_i V_{th}(R_{si} + R_{shi})} \right] \quad (2)$$

in the above equation, $W(X_i)$ is the Lambert W function.

$$X_i = \frac{R_{si}R_{shi}I_{oi}}{nV_{th}(R_{si} + R_{shi})} \exp \left[\frac{R_{shi}(R_{si}I_{phi} + R_{si}I_{oi} + V)}{nV_{th}(R_{si} + R_{shi})} \right] \quad (3)$$

The total output power of PV modules after parallel connection is:

$$P_{all} = P_1 + P_2 \quad (4)$$

When PV modules work at the maximum power point after parallel connection, there are:

$$\frac{\partial P_{all}}{\partial V} |_{V=V_{MP}} = \frac{\partial P_1}{\partial V} |_{V=V_{MP}} + \frac{\partial P_2}{\partial V} |_{V=V_{MP}} = 0 \quad (5)$$

$$\frac{\partial^2 P_{all}}{\partial V^2} |_{V=V_{MP}} = \frac{\partial^2 P_1}{\partial V^2} |_{V=V_{MP}} + \frac{\partial^2 P_2}{\partial V^2} |_{V=V_{MP}} < 0 \quad (6)$$

It is clear that equation (6) holds constantly, and for equation (5) to hold, there are only two cases:

1) $\frac{\partial P_1}{\partial V} |_{V=V_{MP}} > 0$, $\frac{\partial P_2}{\partial V} |_{V=V_{MP}} < 0$ or $\frac{\partial P_1}{\partial V} |_{V=V_{MP}} < 0$, $\frac{\partial P_2}{\partial V} |_{V=V_{MP}} > 0$, as when $P_i < P_{mp(i)}$, that $V_{MP} \neq V_{mp1} \neq V_{mp2}$.

2) $\frac{\partial P_1}{\partial V} |_{V=V_{MP}} = 0$, $\frac{\partial P_2}{\partial V} |_{V=V_{MP}} = 0$, as when $P_i = P_{mp(i)}$, that $V_{MP} = V_{mp1} = V_{mp2}$.

Therefore, within 2 PV modules connected in parallel, only when the V_{mp} of each PV module is equal, the theoretical maximum output power can be obtained. According to previous research^[9], the above conclusions can also be used for PV array parallel mismatch analysis.

2. Detection and reconfiguration methods for PV array parallel mismatch

2.1 Detection methods

After analyzing the mechanism of parallel mismatch, how to quickly and accurately identify the V_{mp} of each PV array becomes the first key problem to be solved. In this paper, we propose a multi-point trigger, short-time I - V curve scanning method, which can quickly obtain the V_{mp} . Compared with the conventional I - V curve scanning method, which has a scanning range from V_{oc} (open circuit voltage) to $0.2V_{oc}$, the scanning interval of the method proposed in this paper is $0.9V_{oc}$ - $0.4V_{oc}$, which can greatly save the scanning time. Since V_{mp} varies with time over a period of 1 day, a multi-point triggered I - V scanning strategy was used to carry out a long-time data acquisition of 1 day in duration and to analyse it.

After obtaining the V_{mp} distribution of the PV array, how to further identify the abnormal PV array is another problem that needs to be addressed. As can be seen from Fig. 3, the parameters that can characterize the change of V_{mp} are: three dimensions including V_{MP_MAX} (maximum value), V_{MP_MIN} (minimum value), and V_{MP_DIF} ($V_{MP_DIF} = V_{MP_MAX} - V_{MP_MIN}$). At the same time, due to the influence factors of the inverter on the sampling accuracy of voltage and current, there is a certain I - V scanning accuracy error. Therefore, it is necessary to further calculate the average value of the V_{mp} distribution after the difference judgment:

$$V_{MP_AVG} = \frac{\sum_{i=1}^n V_{MPi}}{n} \quad (7)$$

In the above equation n is the number of triggered I - V scans. Finally, this paper characterises the abnormal PV array by two feature parameters, V_{MP_AVG} and V_{MP_DIF} .

2.2 Reconfiguration methods

After the abnormal PV array is obtained, it needs to be reconfigured. The essence of reconfiguration is the problem of optimal combination of V_{mp} distribution curves. According to the aforementioned parallel mismatch mechanism, it is clear that the goal of reconstruction is to make the V_{mp} distribution curves of each PV array behave as close as possible, that is, to make each distribution curve align in the time domain as much as possible. Based on this, this paper proposes a method for the root mean square of the V_{mp}

difference to characterize the similarity between the 2 V_{mp} distribution curves using the parameter d obtained from the following equation:

$$d = \frac{\sum_{i=1}^n \sqrt{(V_{mpx(i)} - V_{mpy(i)})^2}}{n} \quad (8)$$

In the above equation, $V_{mpx(i)}$ and $V_{mpy(i)}$ are the two V_{mp} voltages aligned in the time domain, respectively, and n is the number of times the $I-V$ scan is triggered.

3. Testing analysis

3.1 Power station field simulation tests

In order to verify the actual effect of the above methods, a 125KW capacity PV plant platform is built in this paper. PV module type, BPDM60-300WE. The inverter adopts SG125HX [5-ways Maximum Power Point Tracking (MPPT)], both of which are PV arrays with two sinks and one input. Furthermore, simulation tests are carried out under four working conditions (as shown in Figure 2), slight shielding, severe shielding, aging of PV modules (simulated by series resistance), and inconsistent open circuit voltage of PV arrays (simulated by short circuiting PV modules), respectively.



Figure 2. Four test conditions. In order, slight shielding, severe shielding, aging and inconsistent open circuit voltage.

PV arrays corresponding to 5-way MPPT are marked as String1-String10 in order, where String2 simulates severe shielding, String3 simulates inconsistent open circuit voltage, String8 simulates slight shielding, and String10 simulates aging of modules. At the same time, a short-time $I-V$ curve scan is conducted every 1h, with a total of 9 triggers, to obtain the V_{mp} distribution under the 4 sets of simulated operating conditions. Further, by combining the two parameters V_{MP_DIF} and V_{MP_AVG} , the corresponding PV arrays for the four abnormal operating conditions can be identified, respectively.

Table 1 Characterization parameters for PV arrays

	String 1	String 2	String 3	String 4	String 5	String 6	String 7	String 8	String 9	String 10
V_{MP_DIF} (V)	28	224	12	28	16	18	40	105	65	23
V_{MP_AVG} (V)	915	792	793	912	916	910	913	833	913	781

Normal or not Yes No No Yes Yes Yes Yes No Yes No

The *d*-factors are calculated after arranging and combining the strings of the exception groups separately. It is found that String2 and String8 were reconfigured as well as String3 and String10 are reconfigured to have the smallest *d*-factor. Based on this result, the 8-way PV array under this inverter is finally reconfigured and combined, as shown in Table 2. A comparison of the *d*-factors before and after the reconfiguration shows that the *d*-factor is significantly reduced to 72.6% after the reconfiguration.

Table 2 Comparison before and after reconfiguration

Pre-reconfiguration combination	Pre-reconfiguration d-factor	Post-reconfiguration combination	Post-reconfiguration d-factor
String1/ String2	144.2	String1/ String7	14.6
String3/ String4	37.2	String2/ String8	60.3
String7/ String8	91.6	String4/ String9	21.2
String9/ String10	133.4	String3/ String10	15.8
Total	406.4	Total	111.9

Since there are changes in the actual PV plant test environment, such as solar irradiance, before and after the reconfiguration, the evaluation of the reconfiguration effect cannot be directly compared with the power generation or output power before and after the reconfiguration. Therefore, this paper proposes an evaluation method decoupled from solar irradiance, which is calibrated with optimization coefficient *K*, and its definition is as follows, $K = P_m/P_s$.

Where P_m is the actual output power obtained through MPPT and P_s is the sum of the theoretical maximum output power of the 2-way PV array. Then from the above definition, it can be seen that the larger the *K*-coefficient, the better the reconfiguration effect, and the theoretical maximum value of *K*-coefficient is 1. The results obtained for String2 are shown in Fig. 3 for the *K*-coefficients before and after the optimisation. It can be seen that the *K*-coefficients increased by 0.02% to 5.378% after the reconfiguration.

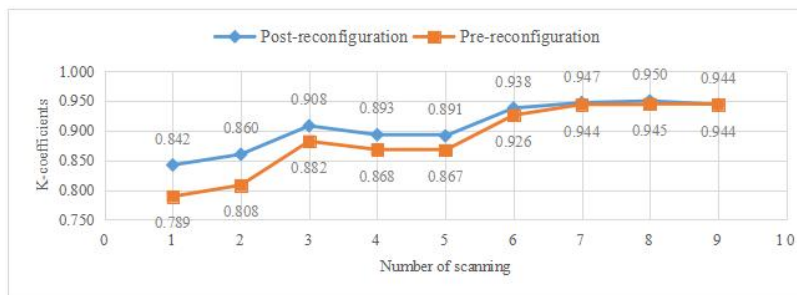


Figure 3. Changes in K coefficient before and after String2 reconfiguration

4. Conclusion

From the mechanism of parallel mismatch, this paper proposes a detection method using short-time $I-V$ scanning and a reconfiguration strategy based on the root mean square of the V_{mp} difference. The simulation tests on PV plants, have achieved good reconfiguration results after characterization by d-parameters and K-coefficients. In summary, the mismatch detection method and reconfiguration strategy derived from the research in this paper are effective in practice.

References

- [1] Fountoukis C, Figgis B, Ackermann L, et al. Effects of atmospheric dust deposition on solar PV energy production in a desert environment[J]. Solar energy, 2018,164: 94-100.
- [2] Styszko K, Jaszczur M, Teneta J, et al. An analysis of the dust deposition on solar photovoltaic modules[J]. Environmental science and pollution research, 2019, 26(9):8393-8401.
- [3] Makkar A, Raheja A, Chawla R, et al. IoT based framework: Mathematical modelling and analysis of dust impact on solar panels[J/OL]. 3D Research, 2019, 10(3-4).
- [4] Fu GX, Li X, Gao XD. Analysis method and application of grid-connected Photovoltaic power Station Based on Current Dispersion rate of bus box Cluster [J]. Power grid and clean energy,2014,30(11):109-113.
- [5] Li M. The Research and Development of Distributed Photovoltaic Power Station Monitoring and Energy Efficiency Analysis System [D]. 2016.
- [6] Chan DSH, Phang JCH. Analytical methods for the extraction of solar-cell single- and double-diode model parameters from $I-V$ characteristics[J]. IEEE Transactions on Electron Devices, 1987, 34(2):286-293.
- [7] Bai J, Cao Y, Hao Y, et al. Characteristic output of PV systems under partial shading or mismatch conditions[J]. Solar Energy, 2015, 112:41-54.
- [8] Ding J. Principle study and technique application of explicit solution for solar cell $I-V$ equation[D].2007.